# Enhancement of Interlaminar Fracture Toughness of Carbon Fiber/Epoxy Composites Using Silk Fibroin Electrospun Nanofibres

## Cuong Manh Vu & Houyng Jin Choi

Accepted author version posted online: 01 Mar 2016.

Submit your article to this journal ↗

View related articles ↗

View Crossmark data ↗

# Enhancement of Interlaminar Fracture Toughness of Carbon fiber/Epoxy Composites using  silk fibroin electrospun nanofibres

Cuong Manh Vu[1,], Houyng Jin Choi[2]

[1]Chemical department, Le Qui Don Technical University,  Ha Noi, Viet Nam

[2]Department of Polymer Science & Engineering, Inha University, Incheon, Korea

Corresponding author. Cuong Manh Vu Email: vumanhcuong309@gmail.com

## Abstract

In this paper, the effect of silk fibroin nanofibres (nSF) as a toughening agent of Carbon fiber/ fabric reinforced Epoxy Composites (CF/EP) is experimentally investigated. The composites showed up to 30% improvement in Mode II fracture toughness the at 0.1 wt.% of nSF content. The scanning electron microscopy (SEM) observation revealed that the fracture surface of nSF modified CF/EP appearance of the broken fiber and the ductile‾like matrix cracks showed a good adhesion between matrix resin and carbon fibers which are reasons for enhance mode II interlaminar fracture toughness.
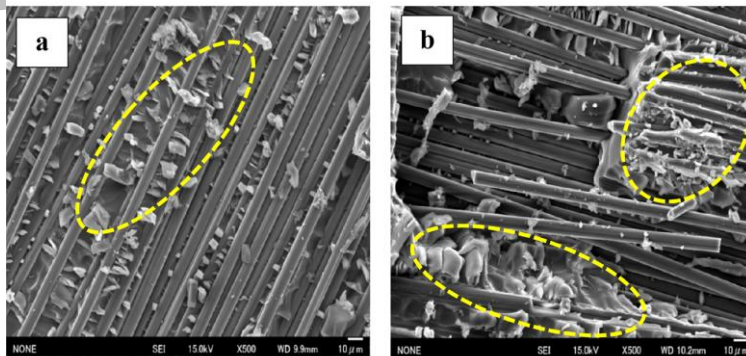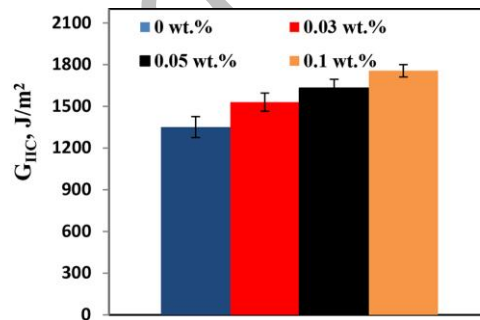
SEM images for the fractured surface of ENF: Unmodified composite (a) and modified composite (b)

**KEYWORDS:** Fracture toughness, silk fibroin nanofibres, CF/EP, electrospinning,

Mode II fracture toughness

## INTRODUCTION

Carbon fiber is one of most important fiber which has been used as reinforced material in

preparing light‾weight composites for structural applications such as aerospace, marine

and automotive because of its superior mechanical properties and low densities. For

preparing fiber reinforced polymer composites (FRP) aims, this fiber is embedded in a

relatively compatible polymer matrix [1]. The most widely used polymeric matrixs are

thermoset epoxies that provide superior thermal, mechanical and electrical properties,

dimensional stability and chemical resistance. However due to intrinsic brittleness of

epoxy matrix after cured that strength properties of CF/EP composites are sensitive to

failure modes such as transverse cracking, longitudinal cracking and delamination

between adjacent layers. Since fiber are mechanically stronger than the matrix [2], the

matrix fracture toughness is the key material property that controls damage initiation and

growth in composites, especially in through‾the‾thickness properties, such as

delamination properties. Delamination is one of the major failure mechanisms associated

with composites that allow cracks to grow between the plies of a laminate. The

investigation before showed that, most epoxy resins are brittle and have Mode I fracture

toughness of about 80–300 J/m$^2$ in the delamination mode [3–5]. Considering delamination

growth from the point of view of fracture mechanics, interlaminar fracture toughness still

plays an important role in damage propagation of CF/EP [6]. In laminate composites based

on epoxy matrix, delamination is strongly related to the brittle nature of epoxy matrix. In

2

this case enhancing the matrix toughness may leads to the improvement of the

interlaminar fracture toughness of laminate composites. Previous work has focused on

enhancing interlaminar fracture toughness of composites by incorporating a small amount

of nano⁻materials (carbon nanotube [7, 8], vapor grow carbon fiber [9, 10], nano⁻cellulose

[11], ...) to the epoxy matrix. In addition, using nanomaterials for the CF/EP composites

could also satisfy the recent demands on the superior performances and more durability

as well as for higher reliability in the fields of advanced applications [12–17].

In this work for modification epoxy matrix the work focused on using nSF as

nanomaterial reinforcer that fabrication by using electrospinning. Electrospinning was

patented by Anton Formhals in 1934 and is a combination of two techniques which are

electrospray and spinning of fibres [18] which has been very interesting for the recent

years for fabrication nanofibers with the help of electrical forces. Silk is an ancient and

the only natural filament fibre which is used for thousands of years and for the year 2011,

China (126 ktons), India (20.4 ktons), Viet Nam (7.05 ktons), Romania (2.1 ktons),

Thailand (1.6 ktons) and Uzbekistan (1.2 ktons) are the six major silk producers in the

world [19]. Silk, is a fine, strong continuous fibroin filament produced by the larva of

certain insects especially the cultured silkworms constructing their cocoons. Raw silk

fibre has natural impurities such as wax, carbohydrates, inorganic matter and pigment

less than 3% wt of a fibre. In a composition of a silk fibre, fibroin content is about 70–

80% and the content of sericin, which is silk gum and usually removed in processing, is

about 20–30% [20]. Silk fibroin polymers contain protein series and are responsible for

cocoon and web formation, nest building, etc. [21, 22]. As they have mostly β⁻sheet

3

structures consisting of short side chain amino acids in the primary sequence, they permit

tight packing of piled sheets of hydrogen bonded anti⁻parallel protein chains. Because of

both large hydrophobic and smaller hydrophilic areas they allow to promote the assembly

of silk which is very good in strength and resiliency [23]. The studies on the silk fibroin

from silkworm cocoons were first reported in 1994 [24]. A hexafluorisopropanol solvent is

used and nano scaled fibres can be produced by the electrospinning process. This process

is similar to the spinning process of a silkworm where the polymer solution is subjected

to a high electric field and this field overcomes the surface tension so polymer ejects,

stretches and deposits a kind of nonwoven mat. Therefore, with this technique the

polymer fibres of micrometres produce fibres in nanometre scales. Nowaday, Silk fibroin

is preffered using for for biomedical application [25–27]. However the using of nSF as

toughness agent for thermoset resin such as EP and CF/EP composites have no published

until now.

The nSF were first prepared by wet electrospinning using methanol bath and then added

to EP using as a matrix for fabrication CF/EP composites by using  methyl

hexahydrophthalic anhydride (MHHPA) as a curing agent. The bonding between cacbon

fibers and EP were accessed by IFSS and interlaminar fracture toughness of CF/EP

composites were accessed by using Mode II fracture toughness. The effect of different

contents of nSF on the morphology and thermo⁻mechanical properties of the prepared

nanocomposites also was examined.

## 1. EXPERIMENTAL

4

### *1.1. Materials*

Silk cocoons were obtained from Vietsilk Limited Company Lam Dong Province, Vietnam was used as nanofiber resource. Besides, lithium bromide (LiBr, Sigma Aldrich), sodium carbonate, methanol, formic acid (Merck, Germany), cellulose dialysis tube (12 KDa, Sigma Aldrich). Plain woven carbon cloth (Toray, Japan). The epoxy resin used is diglycidyl ether of bisphenol A (Epon 828) which was purchased from Shell Chemical and has an epoxide equivalent weight (EEW) of 185⁻192 g/eq. MHHPA purchased from Lindau Chemical (England), was chosen as the curing agent. 1⁻ metyl imidazol (NMI) purchased from BASF (Germany) was used as the accelerator. The chemical structures of DGEBA, MHHPA, NMI and are shown in Figure 1.

### *1.2. Fabrication Of Nsf*

Silk cocoons were boiled in 0.02 M aqueous $Na_2CO_3$ solution for 1 h to remove sericin, washed with deionized water and dried at 37°C overnight. The degummed silk was dissolved in 9.3 M LiBr at 60 °C for 4 hours, dialyzed in a cellulose tube against distilled water for 72 hours and then lyophilized. The prepared SF sponge was then dissolved in formic acid under stirring for 3 hours at room temperature to yield 13 wt% SF solution. Subsequently, the obtained solution was filled in 1 ml syringe with 22 G blunted stainless steel needle. Electrospinning (Electrospinz, New Zealand) was carried out at 20 kV with a constant flow rate of 0.25 ml.h$^{-1}$. The electrospun fibers were collected in the methanol coagulation bath for direct recovery of β⁻sheets. The methanol bath was placed 13 cm under the needle tip. To determine morphology, the fiber mat was attached on an aluminum stub, sputter coated with gold, and imaged with a Scanning Electron

5

Microscope (SEM, Joel JSM 6360, Japan). The morphology of nSF from Figure 2

showed that the nSF was generated with randomly‾aligned fiber web having a diameter

ranging from 50 to 100 nm with concentration 13 wt.%.

### 1.3. Preparation Of CF/EP Composites

nSF was directly mixed into the epoxy resin with different contents (0, 0.03, 0.05, 0.1

wt.%) at $90^0$C for 60 min using a process homogenizer at a rotating speed of 15.000 rpm.

The mixture was then sonicated for 15 min by using an ultrasonic homogenizer. The

curing agent and accelerator were added in the mixture with a molar ratio of

EP/MHHPA/NMI=1/0.87/0.028, after which the mixture was degassed in a vacuum oven

for 15 min. The obtained mixture was hand lay‾upped with plain‾woven carbon fabric

which its fraction of volume was $50 \pm 2\%$ (the volume fraction of EP/CF was 1:1). About

10 layer of CF was used (the thickness of one CF layer equal to 0.4 mm). Curing was

performed at $130^0$C for 1 h and $150^0$C for 1 h in a convection oven.

### 1.4. Resin Fracture Toughness Test

All neat resin and nSF‾modified epoxy resin were cured at $130^0$C for 1 hour and $150^0$C

for 3 hours. The single edge notch bend (SENB) specimen were used to determine the

fracture toughness ($K_{IC}$), as shown in Figure 3 according to ASTM D5045‾99 was

calculated from equation from 1 and 2. The notch tip was machined using a diamond saw.

The pre‾crack was generated using tapping a fresh razor blade. After fabricating SENB

specimens, the crack tip was observed by using the optical microcopy as shown in Figure

4.

6

$$K_{IC} = \left(\frac{P_C}{BW^{1/2}}\right)f(x) \ , \qquad W=2B \qquad (1)$$

$$f(x) = 6x^{1/2}\frac{[1.99 - x(1-x)(2.15 - 3.93x + 2.7x^2)]}{(1+2x)(1-x)^{3/2}} \ , \qquad x=a/W \qquad (2)$$

### *1.5. Interfacial Shear Strength*

To evaluate the effect of nSF on the interfacial shear strength (IFSS) of single carbon fiber and epoxy, micro⁻droplet test was conducted by using Model HM410 instrument carbon single fiber detached from woven fabric, and then was attached to a thin concave plastic or hardboard with double sided adhesive tape or adhesive as were showed in Fig. 5. Epoxy micro⁻droplet with various ratio (0 wt.%, 0.03 wt.%, 0.05 wt.% and 0.1 wt.%) was adhered on a carbon single fiber with an embedded length of 40⁻80 μm by using a fine size applicator. The embedded length was measured using an optical microscopy observation. The IFSS between single fiber with an embedded length of 40⁻80 μm by using a fine size applicator. The embedded length was measured using an optical microscopy observation. The IFSS between single carbon fiber and epoxy was calculated by the following equation:

$$\tau = \frac{F}{\pi D_f L}$$

Where $\tau$ is the interfacial shear strength, F is the critical load, $D_f$ is the single carbon fiber diameter, and L is the embedded length into resin, respectively. At least 20 experiments were tested for each testing specimen.

7

### *1.6. Tensile Test*

The tensile properties of the samples were measured using a Instron 5582⁻100KN

testing machine according to ASTM D3039⁻08. The specimen gage length was 100 mm

and the testing speed was set to 1mm/min. The specimen dimension was 200 mm x 25

mm x 2 mm. Glass fiber reinforced plastic/epoxy tabs or aluminum tabs with thickness of

1.5 mm or 2mm were attached at both ends of the specimen by an adhesive.

### *1.7. Mode⁻II Interlaminar Fracture Toughness Test*

The mode⁻II interlaminar fracture toughness test ($G_{IIC}$) was evaluated by using the

end⁻notch flexural (ENF) test at a loading rate of 1 mm/min as illustrated in Figure. 5

according to JIS K7086 standard. The nominal specimen width (W) was 20 mm, initial

crack length ($a_0$) 25 mm and total specimen length 120 mm. For testing, the specimen

was placed in a three⁻point bending fixture with the haft span length (L) set at a 50 mm

and the ratio ($a_0$/L) maintained at 0.5. Expressions for the calculation of the mode II

critical strain energy release rate ($G_{IIC}$) are derived from the Iwin and Kies expression for

fracture energy:

$$G_{IIC} = \frac{P^2}{2W}\frac{dC}{da} \tag{1}$$

$G_{IIC}$ was calculated by using the direct beam theory method which used the ENF

compliance expression given by Russell and Street.

$$C = \frac{2L^3 + 3a^3}{8EWh^3} \; ; \quad \frac{dC}{da} = \frac{9a^2}{8EWh^3} \; ; \quad E = \frac{2L^3 + 3a^3}{8CWh^3} \tag{2}$$

8

$$G_{IIC} = \frac{9a^2P^2}{16EW^2h^3} \qquad (3).$$

An expression for E can be obtained from (2) which substitutes into Equation (4) (for beam under small defection), yielding:

$$G_{IIC} = \frac{9a^2P\delta}{2W(2L^3 + 3a^3)} \qquad (4)$$

$$a = \left[ \frac{C_1}{C_0}a_0{}^3 + \frac{2}{3}\left(\frac{C_1}{C_0} - 1\right)L^3 \right]^{\frac{1}{3}} \qquad (5)$$

Where Pc is the critical load, C is the compliance (displacement/load; $\delta$/P), W is the width, a is the crack length, E is the flexural modulus of the beam with the absence of pre‾crack, h is half the specimen thickness, $C_1$ is the compliance corresponding to the critical load. $C_0$ is the compliance corresponding to the initial crack, $G_{IIC}$ the critical strain energy release rate.

### 1.8. Dynamic Mechanical Analysis Test

DMA8000 instrument with a chuck distance of 20 mm was used to perform the DMA studies in order to evaluate tan $\delta$ and Tg. DMA gives both the storage modulus and the loss modulus characteristics as a function of temperature. The measurements were carried out at a heating rate of $2^0$C/min from $25^0$C to $250^0$C at fixed frequency of 1 Hz with the three point bending mode. The samples of DMA testing had the approximate dimensions of 40 mm in length, 10 mm in width and 2 mm in thickness.

9

### *1.9. Scanning Electron Microscopy Observations*

The fractured surface of testing specimens were observed by using scanning electron microscopy (SEM⁻JEOL JSM 6360, Japan). Prior to SEM observation, all samples were coated a thin layer of gold to avoid electrical charging.

## 2. RESULTS AND DISCUSSIONS

### *2.1. Resin Fracture Toughness*

The fracture toughness of nSF⁻epoxy with various contents (0 wt.%, 0.03 wt.%, 0.05 wt.%, and 0.1 wt.%) was determined by the three point bending method with SENB specimens. The testing specimens were conducted at the cross⁻head speed of 10 mm/min, which was fast enough to prevent the viscoelastic behavior of the epoxy. The experimental results in Figure 7 showed that The $K_{IC}$ values of epoxy resin were slightly improved with adding nSF. With the addition of 0.1 wt.% of nSF, the fracture toughness was improved by 28.3% from 0.639 MPa.m$^{1/2}$ to 0.82 MPa.m$^{1/2}$. In SEM observation, the smooth fracture surface of the neat epoxy pronounced a typical fracture behavior as shown in Fig 8a. It was noticeable that a smooth mirror⁻like surface, micro⁻flow lines and river pattern was observed. With the addition of nSF, the roughness fracture surface was revealed suggesting the crack propagation could be delayed so that more energy was required. This could be attributed the crack encountered nano⁻fibers bridging as shown in Fig 8b.

### *2.2. Micro⁻Droplet Test*

10

The interfacial shear strength (IFSS) between fiber and matrix have been strongly affected by the presence of nanofibers, such as carbon nanotube, nanoclay, nanosilica, etc. [28–30]. In this study, the micro⁻droplet test was used to evaluate the IFSS of single carbon fiber and epoxy droplets with the addition of nSF. Fig. 9 showed that the IFSS gradually enhanced with an increase of nSF content. The IFSS value of the modified composite at 0, 0.03, 0.05, 0.1 wt.% of nSF were 59.45, 62.39, 68.54 and 71.44 MPa. It mean that, at 0.1 wt.% of nSF content, the IFSS strongly increased by 20%. The IFSS value of the modified composite at 0.1 wt.% nSF was increased from 59.45 MPa to 71.44 MPa.. It found that the role of nSF contributed to relatively improve of interphase between single carbon fiber and epoxy.

### 2.3. Tensile Test

The effect of nSF contents on the mechanical behavior of the CF/EP composites was investigated. For the modified composite, the tensile strength and Young`s modulus slightly increased with the addition of nSF contents as summarized in Fig. 10. It was worth noting that at 0.05 wt.% nSF, the tensile strength for the modified composite increased by 4.8% higher than that of the unmodified composite. It is pronounced that the addition of nano⁻materials plays an important role in improving the strength of the interface. This could be attributing to the dependence of the tensile strength of the nanoreinforced interface to the nanosized fillers which characterized by large surface areas per unit gram. Thus, addition of small amount of nSF leading to the number of adhesively jointed points with carbon fibers was very low which had no effect on the tensile strength of the CF/EP composites.

11

### *2.4. Mode‾II Interlaminar Fracture Toughness Test*

In the end notch flexure (ENF) test, the specimen is loaded in a three point flexural fixture as shown in Fig. 6. The experimental results of Fig.11 showed a plot of the interlaminar fracture toughness of the CF/EP composites as a function of nSF of content. With the gradual addition of nSF content, the critical energy release ($G_{IIC}$) also gradually increased. At 0.1 wt.% nSF, the $G_{IIC}$ increased by 30%. It was worth nothing that the fracture toughness of the CF/EP composites increased from the energy‾dissipating events, such as fiber matrix debonding, fiber pull‾out and bridging as well as the fracturing of the matrix and fibers [31–33]. The fractured surfaces of ENF specimens were examined using SEM. Fig. 12 (a) showed that the sheared hackle markings in the epoxy matrix, which was characteristic of brittle fracture. Moreover, there was almost no broken fiber bridging, and the cracks propagated along the fiber‾matrix. It showed that the adhesion between resin and carbon fiber was relatively weak. On the other hand, Fig. 12 (b) with the appearance of the broken fiber and the ductile‾like matrix cracks showed a good adhesion between matrix resin and carbon fibers. This could be attributed to the tougher matrix when incorporated nSF. The higher toughness was achieved due to micro/nano‾cracks pined via forming nanofiber bridging. It considered that such reasons improved the critical energy release rate.

### *2.5. Dynamic Mechanical Analysis Test*

Effect of nSF on the thermal mechanical behavior of the CF/EP composites was determined using dynamic mechanical analysis (DMA). The results in Fig. 13 (a) showed that the glass transition temperature ($T_g$) of the composite with various contents of nSF (0

wt.%, 0.03 wt.%, 0.05 wt.% and 0.1 wt.%) were $165.3^0C$, $162.03^0C$, $161.01^0C$ and $160.83^0C$, respectively. It found that there was a tendency for the slight decrease of Tg in the composite with the presence of nSF. On the other hand, the addition of nSF affected the damping of the CF/EP composites through the determination of the loss tangent value (tan δ), namely the tan δ values of the modified composite was lower than that of the unmodified composite. The tan δ value of 0.1 wt.% nSF decreased by 15% from 0.5744 to 0.4882. This can be related to the non⁻dissipative nature of the filler, which reduces the viscolelastic response of the composite. The results in Fig. 13 (b) performed that the storage modulus of the CF/EP composites slightly increased with an increase of nSF content. The addition of 0.1 wt% of nSF yielded a 5.75% increase of the storage modulus at $25^0C$. These results confirmed that the incorporation of nSF improvement of the stiffness of the composite.

## 3. CONCLUSIONS

In this study, we investigated how to fabricate randomly–aligned web of SF nanofibers form the electrospinning process. The effects of nSF on the mechanical properties of the CF/EP composites were determined.

⁻ The fracture toughness of nSF⁻epoxy was improved by 28.3% with the addition of 0.1 wt.% nSF.

⁻ The incorporation of 0.1wt.% nSF contributed to improvement of the IFSS between single carbon fiber and micro⁻droplet epoxy with an increase by 20%.

⁻ There was a slight increase of the tensile strength by about 5% with the addition of 0.05 wt.% nSF.

⁻ There was an increase of the mode⁻II interlaminar fracture toughness ($G_{IIC}$) at 0.1wt.% nSF by 30%.

## REFERENCES

1.    Jin Z, Khunlavit C, Shuai H, Chun H., Wang. Hybrid composite laminates reinforced with glass/carbon woven fabrics for lightweight load bearing structures. Materials and Design 2011; 36: 75 ⁻ 80.

2.    Hull D. An introduction to composite materials. Cambridge University Press; 1981.

3.    Garg A, Ishai O. Hygrothermal influence on delamination behavior of graphite/epoxy laminates. Eng Fract Mech 1985; 22(3):413–27.

4.    Keary PE et al. Mode I interlaminar fracture toughness of composites using slender double cantilevered beam specimens. J Compos Mater 1985;19:154–77.

5.    Whitney JM, Browning CE, Hoogsteden W. A Double cantilever beam test for characterizing Mode I delamination of composite materials. J Reinf Plast Compos 1982;1(4):297–313.

6.    Masahiro A, Tatsuya S, Satoshi H, Hiroaki I, Ning H, Marino Q. Mixed modes interlaminar fracture toughness of CFRP laminates toughness with CNF interlayer, Acta Mechanica Solida Sinica. 2012; 25(3):322.

7.    Yokozeki T, Iwahori Y, Ishibashi M, Yanagisawa T, Imai K, Arai M, et al. Fracture toughness improvement of CFRP laminates by dispersion of cup⁻stacked carbon nanotubes. Compos Sci Technol 2009;69(14):2268–73.

8.  Lee S⁻H, Kim H, Hang S, Cheong S⁻K. Interlaminar fracture toughness of composite laminates with CNT⁻enhanced nonwoven carbon tissue interleave. Compos Sci Technol 2012;73:1–8.

9.  Li Y, Hori N, Arai M, Hu N, Liu Y, Fukunaga H. Improvement of interlaminar mechanical properties of CFRP laminates using VGCF. Compos A Appl Sci Manuf 2009;40(12):2004–12.

10.  Arai M, Noro Y, Sugimoto K⁻i, Endo M. Mode I and mode II interlaminar fracture toughness of CFRP laminates toughened by carbon nanofiber interlayer. Compos Sci Technol 2008;68(2):516–25.

11.  Mohamed H. Gabr, Nguyen T. Phong, Kazuya Okubo, Kiyoshi Uzawa,Isao Kimpara, Toru Fujii Thermal and mechanical properties of electrospun nano⁻celullose reinforced epoxy nanocomposites Polymer Testing 2014; 37:51– 58.

12.  Doris W.Y.W, Lin L, P. Terry McCrail, Ton P, Paul J. H. Improved fracture toughness of carbon fibre/epoxy composite laminates using dissolvable thermoplastic fibres. Composites: Part A. 2010; 41:759⁻67.

13.  Ke W, Ling C, Jingshen W, Mei L.T, Chaobin H, and Albert F.Y. Epoxy Nanocomposites with Highly Exfoliated Clay:    Mechanical Properties and Fracture Mechanisms. Macromolecules. 2005; 38:788⁻800.

14.  S Alessi, D Conduruta, G Pitarresi, C Dispenza, G Spadaro. Accelerated ageing due to moisture absorption of thermally cured epoxy resin/polyethersulphone blends. Thermal, mechanical and morphological behaviour. Polymer Degradation and Stability. 2011; 96:642⁻648.

15

15.    Hiroaki M, Michael J.R, Lawrence T.D. Thermo⁻physical properties of epoxy

nanocomposites reinforced by carbon nanotubes and vapor grown carbon fibers.

Thermochimica Acta. 2006; 442:67⁻73.

16.    Ashish W, Ajay G, Olivier R, Luca M, Frederic L, Larissa G, Stephan V.L, Aart

W.V.V, Ignaas V. The effect of adding carbon nanotubes to glass/epoxy composites in

the fibre sizing and/or the matrix. Composites Part A: Applied Science and

Manufacturing 2010; 41(4):532⁻8.

17.    Naveed A. S, Ricky S.C. W, Jang K. K, Christopher C.K.L, Arshad M. Mode I

interlaminar fracture behavior and mechanical properties of CFRPs with nanoclay⁻filled

epoxy matrix. Composite: Part A 2007; 38, :449⁻60.

18.    J.D. Schiffman, C.L. Schauer. A Review: Electrospinning of Biopolymer

Nanofibers and their Applications Polym. Rev 2008; 48 (2):317–352.

19.    S. Muge Y, Nihal S, Suat C. Biomaterial applications of silk fibroin electrospun

nanofibres. Microelectronic Engineering 2015; 146: 43–47.

20.    M.L. Gulrajani, Rev. Prog. Color. Relat. Top. 22 (1) (1992) 79–89.

21.    D.L. Kaplan, S.M. Mello, S. Arcidiacono, S. Fossey, K.W.M. Senecal, Protein

Based Materials, Birkhauser, Boston, 1998; 323:103–131.

22.    P. Wong, C. Foo, D.L. Kaplan. Genetic engineering of fibrous proteins: spider

dragline silk and collagen. Adv. Drug Deliv. Rev 2002; 54 (8):1131–1143.

23.    J. Perez⁻Rigueiro, C. Viney, J. Llorca, M. Elices. Mechanical properties of single⁻

brin silkworm silk. J. Appl. Polym. Sci 2000; 75:1270–1277.

24.    J. Cappello, K.P. MacGrath, C. Viney, in: D. Kaplan, W. Adam, B. Farmer (Eds.),

Spinning of Protein Polymers Fibers, ACS, Washington, DC, 1994, pp. 311–327

16

25. F. Han, S. Liu, X. Liu, Y. Pei, S. Bai, H. Zhao, Q. Lu, F. Ma, D.L. Kaplan, H. Zhu. Woven silk fabric‾reinforced silk nanofibrous scaffolds for regenerating load‾bearing soft tissues. Acta Biomater 2014; 10:921–930.

26.    Q. Lu, X.L. Wang, S.Z. Lu, M.Z. Li, D.L. Kaplan, H.S. Zhu. Nanofibrous architecture of silk fibroin scaffolds prepared with a mild self‾assembly process. Biomaterials 2011; 32:1059–1067.

27.    B. Kundi, N.E. Kurland, S. Bano, C. Patra, F.B. Engel, V.K. Yadavalli, S.C. Kundu. Silk proteins for biomedical applications: Bioengineering perspectives. Prog. Polym. Sci, 2014;39: 251–267.

28.    Li Y, Thomas W. H, Anthony G.E, Gary L. B, David. G. S, and Gary E. W. Electrospinning and Stabilization of Fully Hydrolyzed Poly(Vinyl Alcohol) Fibers. Chemistry of Materials 2003; 15: 1860‾4.

29.    Bin D, Hak Y.K, Se C.L, Douk‾R.L, and Kyung J.C. Preparation and characterization of nanoscaled poly(vinyl alcohol) fibers via electrospinning. Fibers and Polymers 2002; 3:73‾9.

30.    Surawut C, Pitt S. Fabrication of Aligned Poly(vinyl alcohol) Nanofibers by Electrospinning Journal of Nanoscience and Nanotechnology 2006; 6:125‾9.

31.    Masanobu H, Ken‾ichi T, Toru F. Strength and damage accumulation of carbon fabric composites with a cross‾linked NBR modified epoxy under static and cyclic loadings. Composite Structure 1995;32:357‾66.

32.    Yasuhiro N, Kazuya O, Toru F, Kazumasa K. Fatigue crack constraint in plain‾woven CFRP using newly‾developed spread tows. International Journal of Fatigue 2006;  28:1248‾53.

17

33.     Shafi U.K, Arshad M, Rizwan H, Jang‐Kyo K. Fatigue damage behaviours of carbon

fiber‐reinforced epoxy composite. Composite Science and Technology 2010; 70: 2077‐85.

**Figure 1**: Chemical structures of the materials used



MHHPA



NMI
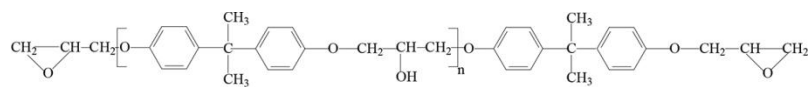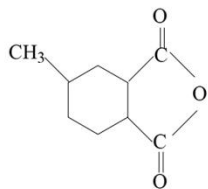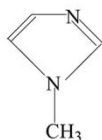
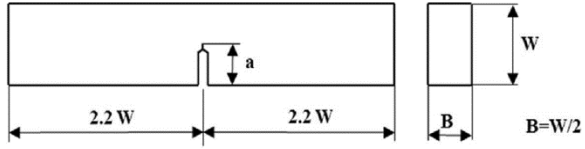**Figure 2**: The morphology of nSF

20
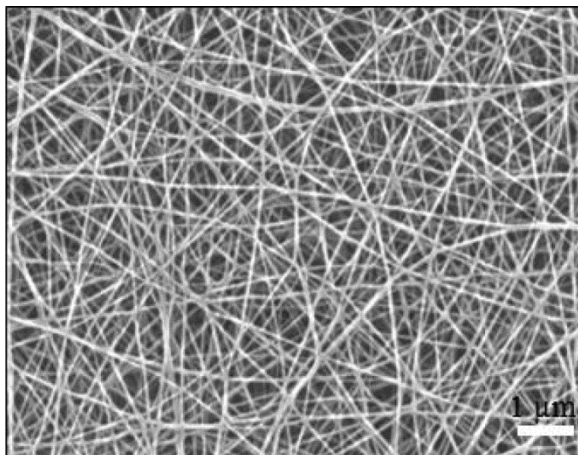
**Figure 3**.  Dimension of the single edge notched bending specimen

21

**Figure. 4**. (a) The initial notch, (b) A pre-crack using a fresh razor blade
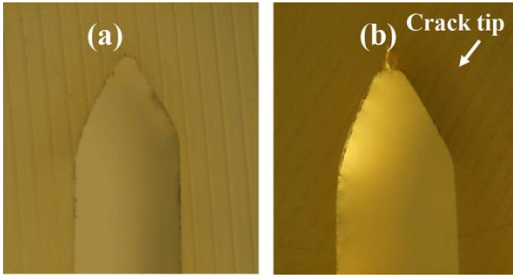
**Figure. 5**. Experimental arrangement for the micro-droplet test: (a) Schematic drawing for the IFSS test; (b) Micro-droplet specimen.



23
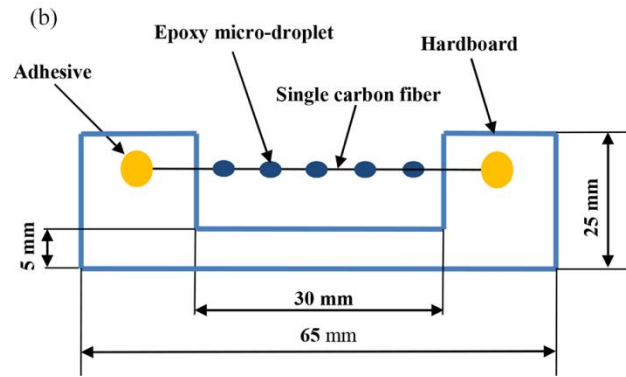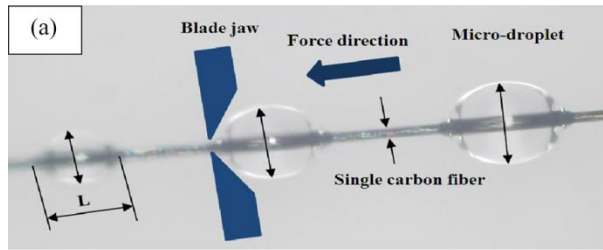
**Figure. 6.** Mode II specimen geometry.
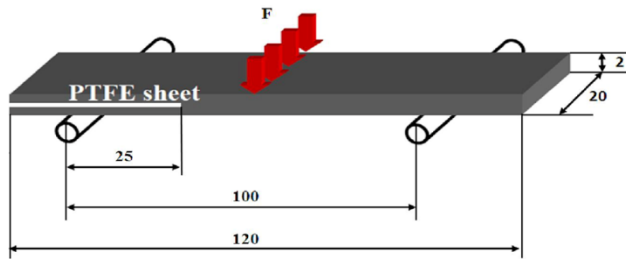
**Figure. 7**. Fracture toughness of the epoxy with various nSF contents.

25
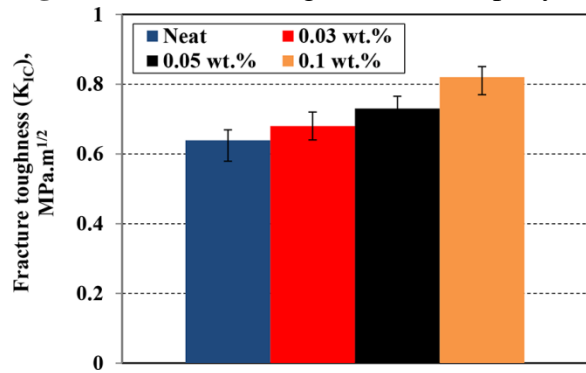
**Figure 8:** SEM images of the epoxy for fracture toughness test with various contents: (a) neat epoxy; (b) 0.1 wt.% of nSF.
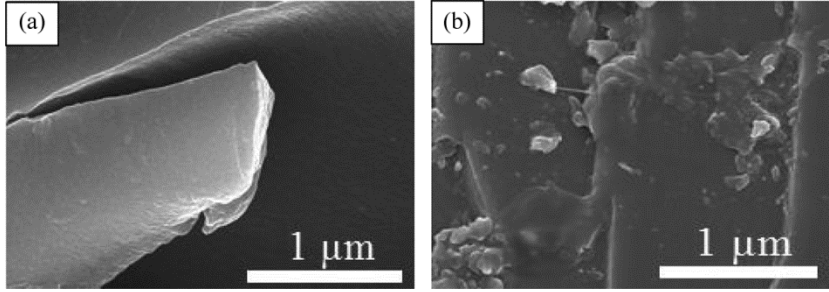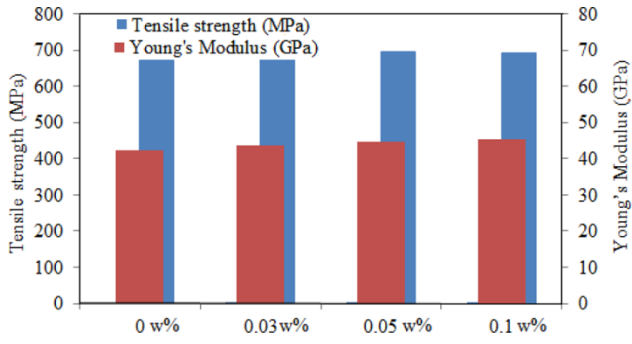
**Figure 9:** Interfacial shear strength of single carbon fiber and epoxy with various nSF contents.



27
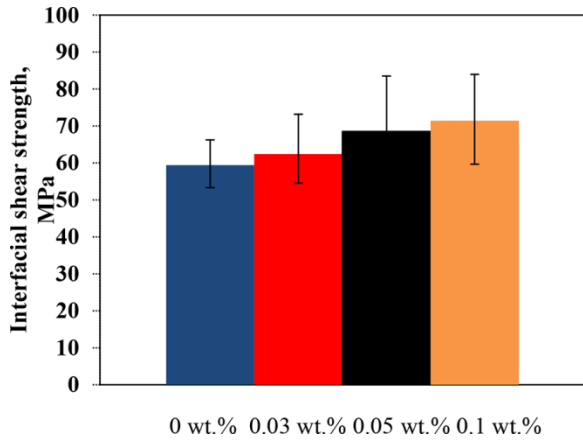
**Figure.10**. Tensile strength and Young's Modulus of the CF/EP composites with various nSF contents.

**Figure. 11**: Critical energy release rate ($G_{IIC}$) for various nSF contents.
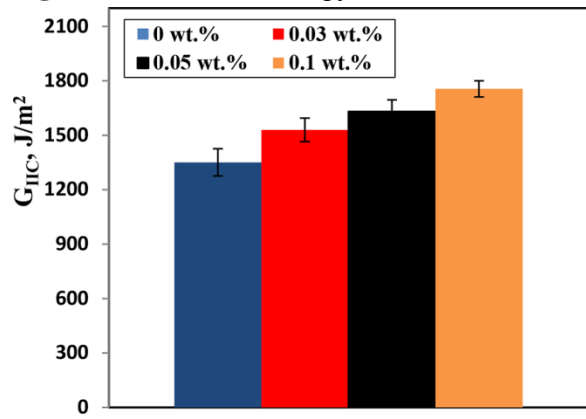
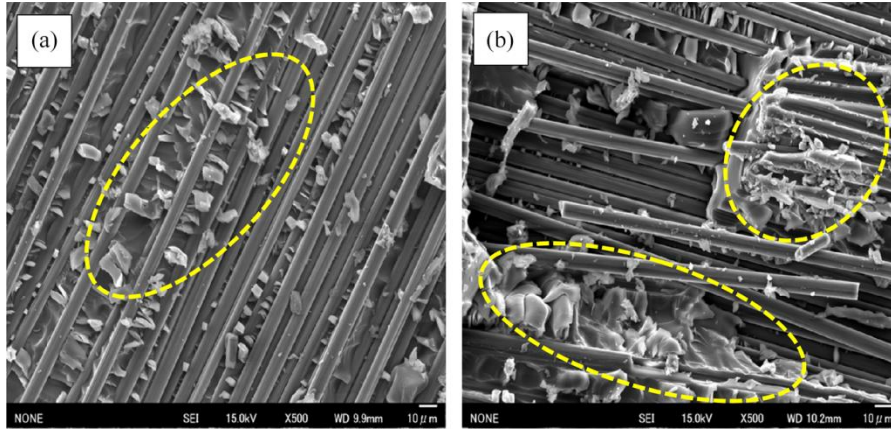**Figure. 12**. SEM images for the fractured surface of ENF test: (a) unmodified , (b) modified.

30

**Figure. 13**: Loss tangent (tan δ) (a) and Storage modulus versus temperature (b) for the CF/EP composites with various contents of nSF.

31